CDK9 recruits HUWE1 E3 ligase to degrade RARα in a kinase independent manner and offers therapeutic opportunities for cutaneous T-cell lymphoma

Supplemental Figures

Supplemental Fig. 1 CDK9 is overexpressed in CTCL.

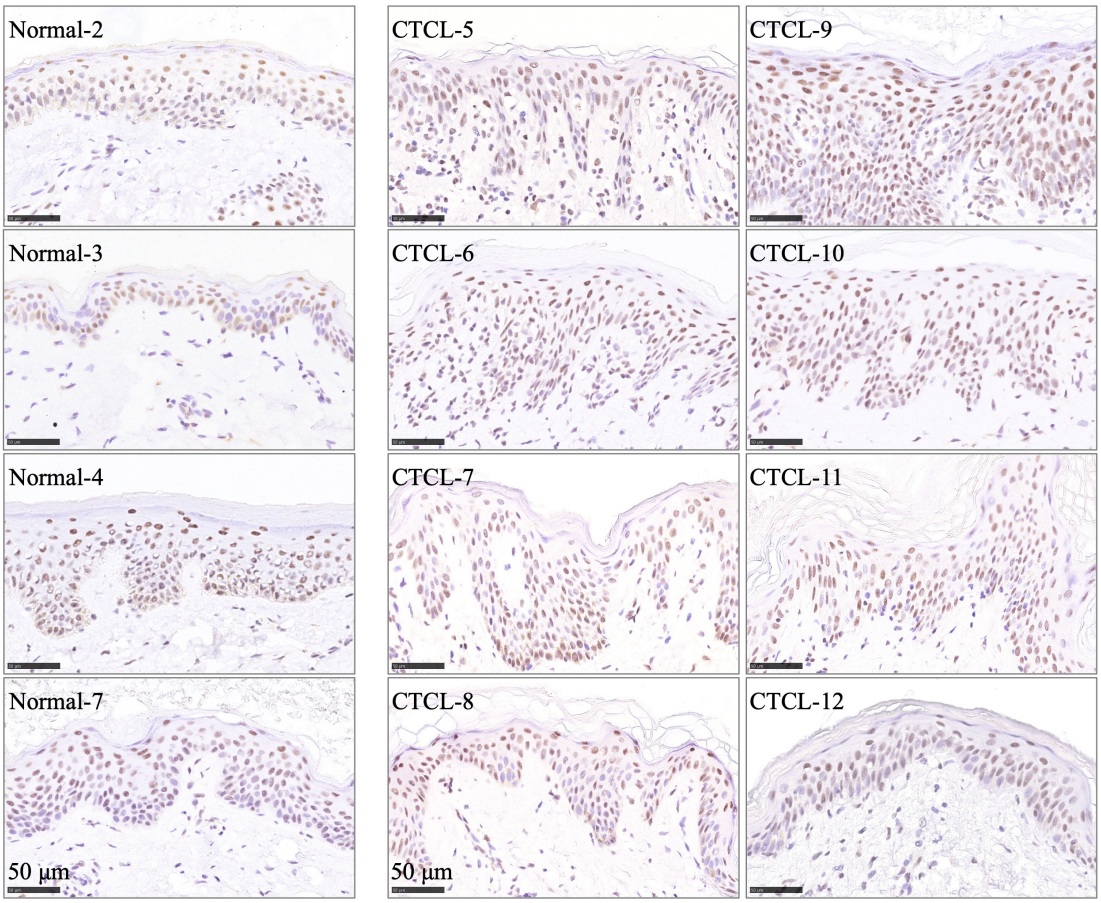

Supplemental Figure 1

Immunohistochemistry (IHC) assay was performed using antibody against CDK9 on samples collected from healthy donors (Normal) or CTCL patients.

Supplemental Fig. 2 CDK9 is overexpressed in specific CTCL cell cluster.

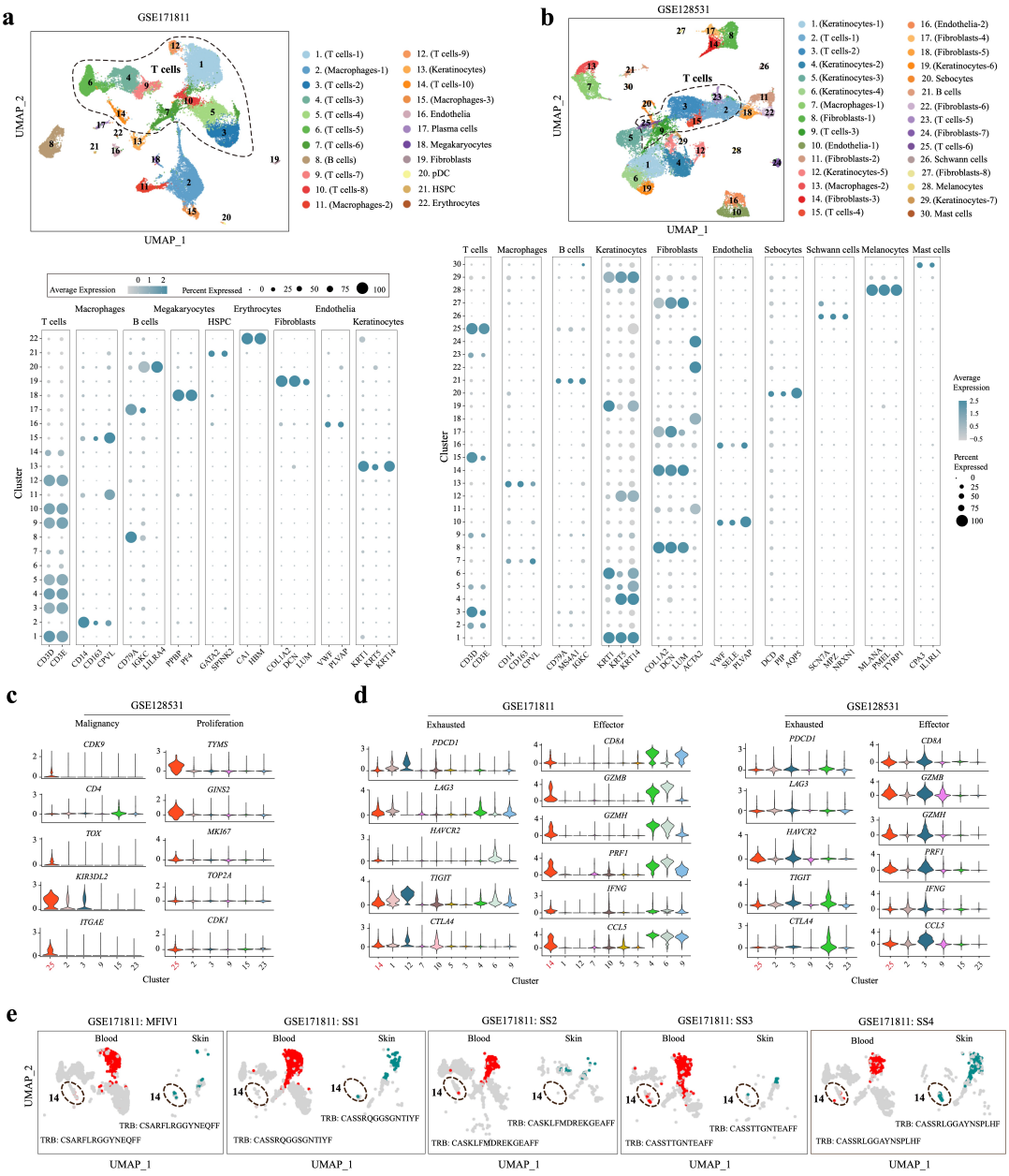

Supplemental Figure 2

a, UMAP projection (top panel) and Dot plot (bottom panel) of GSE171811 including blood cells from 2 Sézary syndrome (SS) patients, matched skin and blood cells from 5 SS and leukemic Mycosis Fungoides (MF) patients and a healthy control (HC). **b**, UMAP projection (top panel) and Dot plot (bottom panel) of GSE128531 including skin cells from 5 CTCL patients and 4 HCs. **c**, Violin plots of T cell clusters in GSE128531 showing the specific expression of CDK9 and proliferating markers. **d**, Violin plots of T cell clusters in GSE171811 and GSE128531 exhibiting the expression levels of exhausted genes (left panel) and effector genes (right panel). CDK9^{high} cluster number was labeled in red. **e**, UMAP representation split by tissues of T cells from GSE171811. Malignant T cells from skin and blood are colored by dark cyan and red, the other T cells are labeled in grey. CDK9^{high} cluster number was labeled using the bold black text and cells were indicated by the dotted oval.

Supplemental Fig. 3 Evaluation of different SNS-032-based PROTACs on CTCL cells.

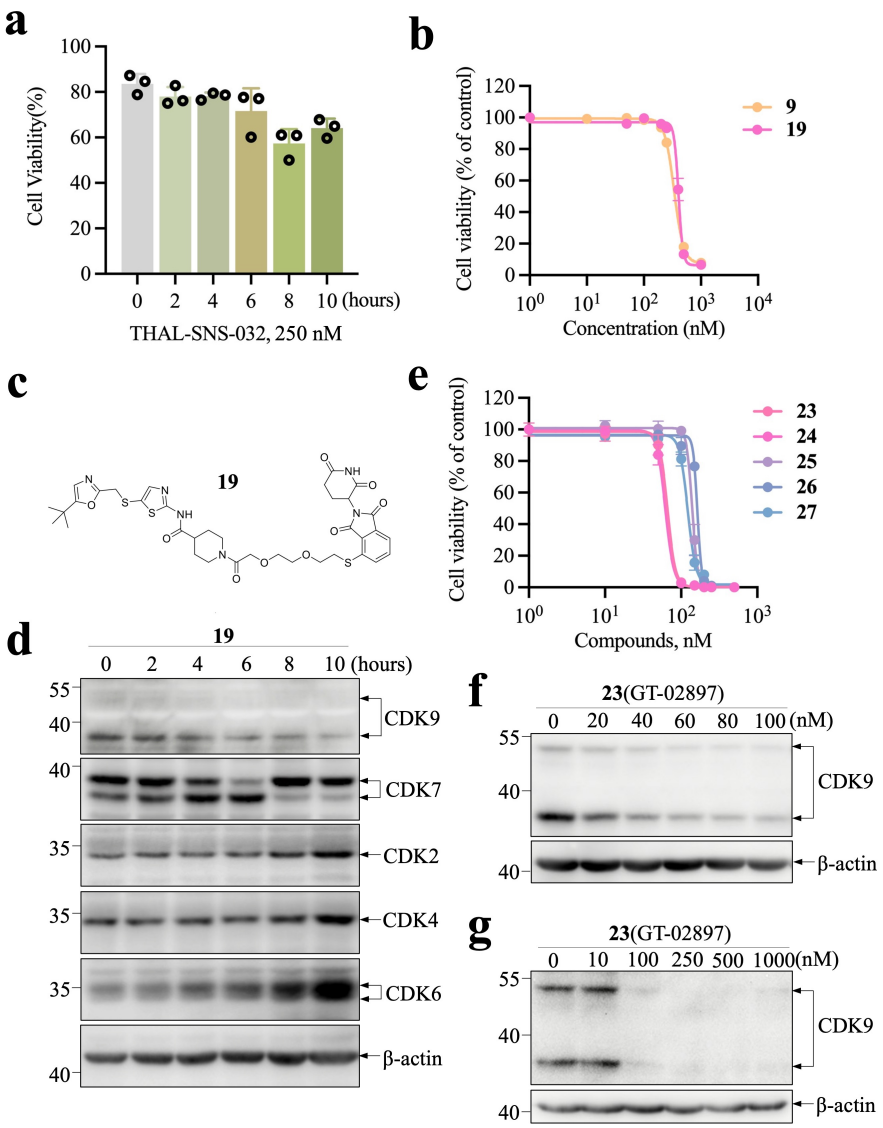

Supplemental Figure 3

a, Hut78 cells were treated with 250 nM THAL-SNS-032 and the cell death were measured by trypan blue staining. **b**, Hut78 cells were treated with indicated PROTACs from 1 nM to 1 μM and the IC_{50} curves were drawn. **c**, Chemical structure of **19**. **d**, Western blot analysis of indicated proteins in HH cells upon **19** (250 nM) treatment for indicated hours. **e**, Hut78 cells were treated with indicated PROTACs from 1 nM to 1 μM and the IC_{50} curves were drawn. **f**, **g**, Western blot analysis of indicated proteins in EL4 cells upon 24 h of DMSO or **23** (GT-02897) treatment at indicated concentrations.

Supplemental Fig. 4 Pathways modulated by ATRA in three different cell lines.

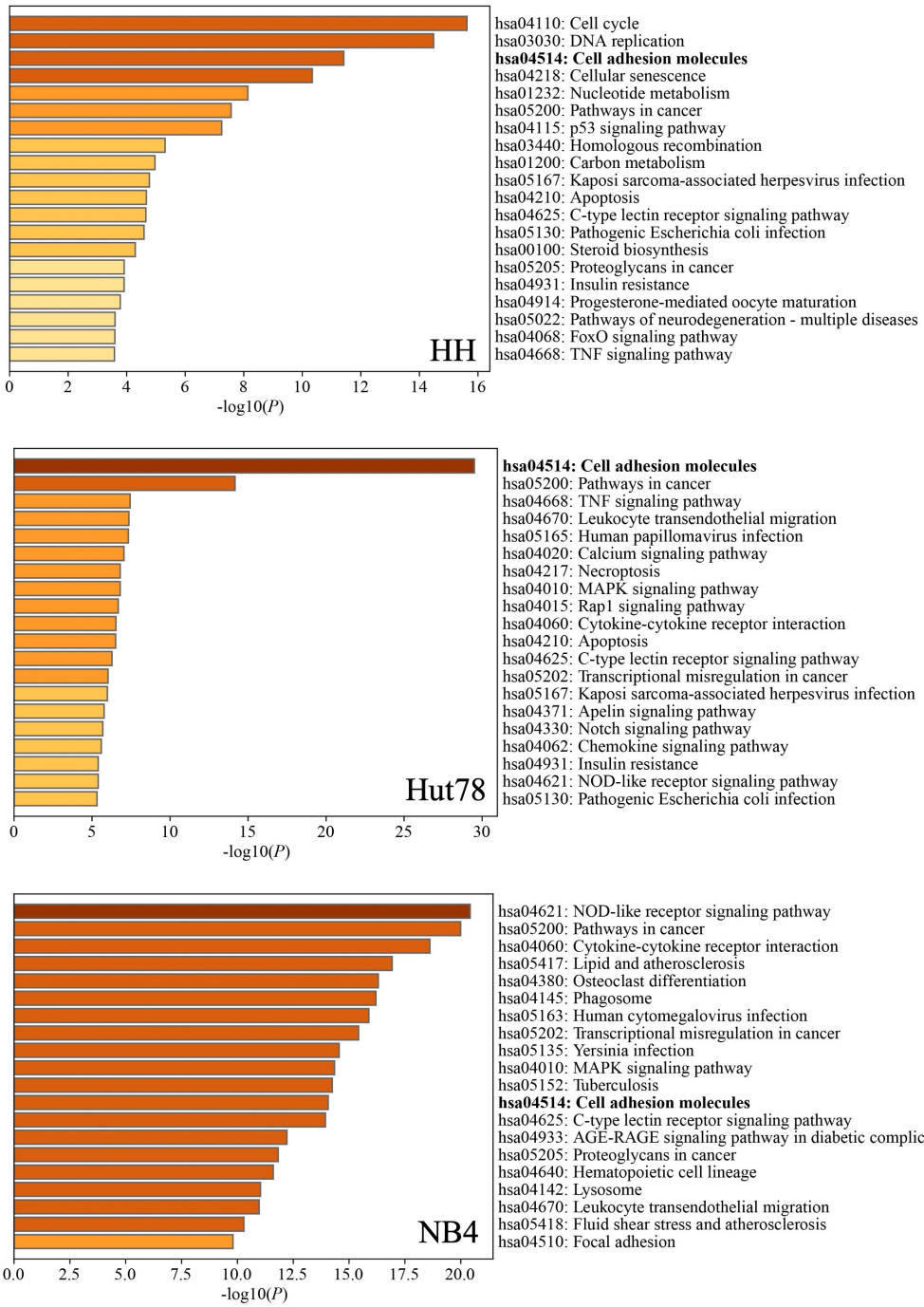

Supplemental Figure 4

HH, Hut78 and NB4 cells were treated with 1 μM ATRA for 6 h and RNA-seq were performed. Data were analyzed for the most significant pathways represented using Metascape.

Supplemental Fig. 5 ATRA does not alter Foxp3 expression in CTCL cells.

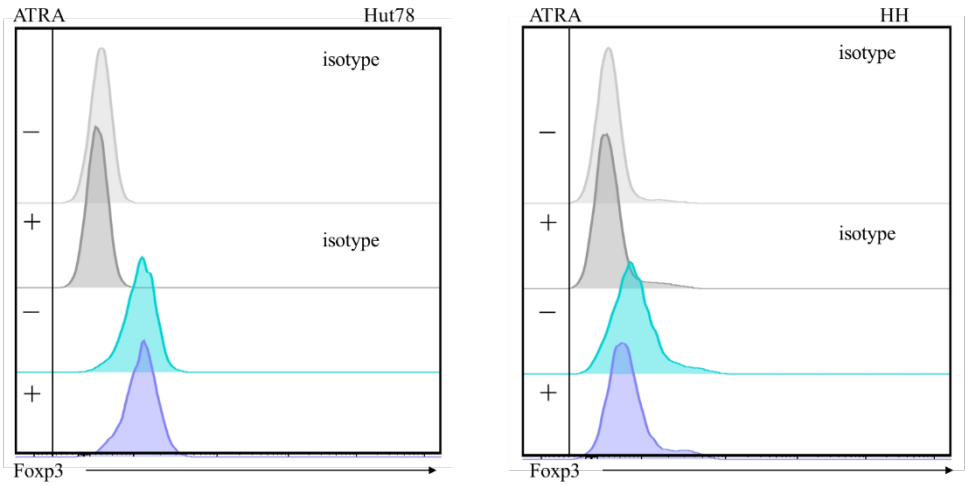

Supplemental Figure 5

Hut78 or HH cells were seeded at 5×10^5 cells/ml before treatment and counted by trypan blue exclusion staining. Then the cells were treated with ATRA (1 μM) or DMSO for 48 h and Foxp3 expression was analyzed by flow cytometry using antibodies against Foxp3.

Supplemental Fig. 6 ATRA displays synergistic effects with GT-02897 in the treatment of CTCL.

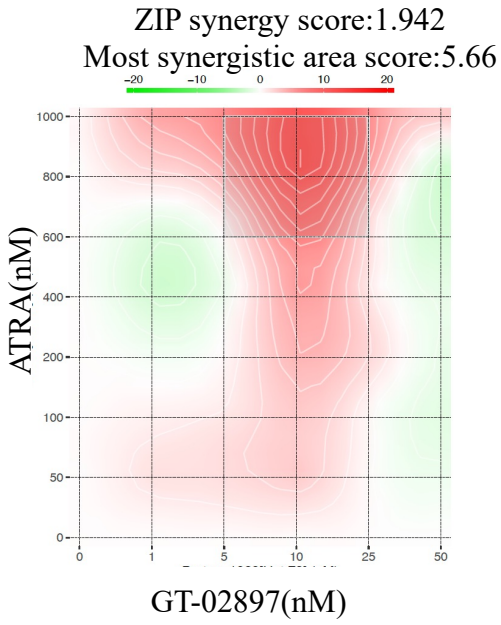

Supplemental Figure 6

Hut78 cells were treated with ATRA (0, 50, 100, 200, 400, 600, 800 and 1000 nM) and GT-02897 (0, 1, 5, 10, 25 and 50 nM) alone or combined for 48 h. At the end of the incubation period, viability was measured by trypan blue. Synergy plot was derived using ZIP method. Image represents one replicate performed in duplicate.

Supplemental Methods

Compound library screening

The small molecular inhibitors library (Selleckchem L1200) and the CDK inhibitors library (MedChemExpress, HYCPK9807, HYCPK9808, HYCPK9809, HYCPK9810) were applied. Cells were seeded into 96-well plates at 100000 cells/ml, and inhibitors were added at 2 μM final concentration. Cell viability was measured 48 h post treatment using the CCK8 kit (CK04, Dojindo).

Patient samples and cell cultures

Primary samples were collected from CTCL patients or healthy donors at Department of Hematology of the Second Hospital of Dalian Medical University. All patients and healthy donors provided written consent to protocols that were approved by the Institutional Review Board and Medical Science Ethic Committee of Dalian Medical University in accordance with the Declaration of Helsinki, which enabled identified research use of biospecimens. Human Peripheral Blood Mononuclear Cells (PBMCs) were prepared from healthy donors' blood using Ficoll Hypaque (1114547, Axis-Shield) density centrifugation. Primary T cells were isolated from the PBMCs using an EasySep Human CD3 Positive Selection Kit (17851, STEMCELL Technologies, Canada) according to the manufacturer's instructions. Human CTCL cell lines (HH, Hut78 and MJ), mouse T cell lymphoma cell line EL4 and human embryonal kidney cell line 293T were purchased from ATCC. Mouse embryonic fibroblasts MEFs were gifted by Professor Zhangjing[1]. HH, Hut78, MJ and EL4 cells were cultured in complete RPMI 1640 medium supplemented with 10% fetal bovine serum (FBS, Sigma)

and maintained in a humidified atmosphere of 5% CO_2 at 37 °C. 293T and MEF cells were cultured in complete DMEM supplemented with 10% FBS (Sigma).

IC_{50} (half-maximal inhibitory concentration) assay

The IC_{50} was defined as the concentration of an inhibitor that reduced cell survival to 50% of the untreated control value, with the highest viability (no inhibitor) defined as 100%, and the lowest viability defined as 0%. HH and Hut78 cells were seeded (1×10^5 cells/ml) in 6-well plates. Cell number and viability were determined after 48 h treatment with different compounds at indicated concentrations by trypan blue exclusion count and compared with untreated control. Mean ± SD of n = 3 biological replicates. Calculation of IC_{50} values was performed using GraphPad Prism version 9.3.1. (GraphPad Software, Inc.).

Cell proliferation assays

Cells were counted on day 0 by trypan blue exclusion and plated in 6-well plates at 1×10^5 cells/ml. Cell counts were then determined by trypan blue exclusion every day and normalized to value of day 0.

Western blotting

Protein extracts were equally loaded on SDS-polyacrylamide gel, transferred to nitrocellulose membrane (HATF00010, Merck Millipore), blocked by 2% (w/v) BSA, and immunoblotted with the indicated antibodies. Post incubation with horseradish peroxidase (HRP)-linked second antibody (Cell Signaling, Beverly, MA) at room temperature for 1 h, projection was performed using Immobilon Western

Chemiluminescent HRP substrate kit (WBKLS0500, Merck Millipore) according to the manufacturer's instructions.

Immunoprecipitation

Cells were harvested and lysed with NP-40 lysis buffer (P0013F, Beyotime) containing 1 mM PMSF and 1× protease inhibitor cocktail (L-1009, BioTNT). After sonication, the supernatants (whole cell lysates) were collected by centrifugation at 20,000 × ***g*** for 10 min at 4 °C and then incubated with anti-Flag M2 Affinity Isolated Antibody (M8823, Sigma-Aldrich) or anti-HA Magnetic Agarose Beads (L-1009, BioTNT) for immunoprecipitation of Flag or HA-tagged proteins. The tubes were slightly rotated overnight at 4 °C, followed by separating the supernatants with a magnetic separator. For immunoprecipitation of RARα, after pre-cleared with protein A/G-agarose beads (sc-2003, Santa Cruz, CA), supernatants were incubated with RARα antibody overnight and protein A/G-agarose beads for 4 h at 4 °C. All precipitates were washed three times with NP-40 lysis buffer and boiled in 1 × loading buffer before western blot analysis.

Denaturing ubiquitination assay

293T cells were treated with 10 μM of the proteasome inhibitor MG132 for 6 h, harvested and lysed with denature lysis buffer (denatured IP buffer 50 mM Tris-HCl, pH 6.8, 2% SDS) by boiling at 100 °C for 20 min to dissociate protein-protein interactions. After centrifugation at 20,000 × ***g*** for 10 min at 4 °C, 140 μl of supernatants was diluted by 1.26 ml NP-40 lysis buffer containing 1 mM PMSF and 1× protease inhibitor cocktail (L-1009, BioTNT) and subjected to immunoprecipitation

with anti-HA Magnetic Agarose Beads (BioTNT), followed by Western blot analysis to visualize polyubiquitylated protein bands.

Real-time RT-PCR (Reverse Transcription-Polymerase Chain Reaction)

Total RNA was extracted from HH and Hut78 cells by TRIzol reagent (Invitrogen), and RT was performed by FastKing RT Kit (TIANGEN, KR116) following the manufacturer's instructions.

The human *β-actin* housekeeping gene was used as an internal control (F: 5'-CATCCTCACCCTGAAGTACCC-3', R: 5'-AGCCTGGATAGCAACGTACATG-3'). Real-time RT-PCR was performed using SYBR Selected Master Mix (Thermo Fisher Scientific, 447308) on QuantStudio 5 instrument (Applied Biosystems) using a primer-specific standard curve with denaturation (95 °C for 10 min), amplification repeated 40 times (95 °C for 15 s, 60 °C for 1 min). For each sample, ddCt (crossing point) values were calculated as the Ct of the target gene minus the Ct of the actin gene.

Human *CDK9*-F: 5'-CCAGAAGCGGAAGGTGAA-3', Human *CDK9*-R: 5'-CCAGAAGAAGTCGTGGTTGAG-3'.

Human *RARα*-F: 5'-AAGCCCGAGTGCTCTGAGA-3', Human *RARα*-R: 5'-TTCGTAGTGTATTTGCCCAGC-3'.

Human *STAT4*-F: 5'-TGTTGGCCCAATGGATTGAAA-3', Human *STAT4*-R: 5'-GGAAACACGACCTAACTGTTCAT-3'.

Human *IL12RB1*-F: 5'-AGCTGCGTATGGAGTGGGA-3', Human *IL12RB1*-R: 5'-GAGGCAGGACTCAGTATCATCA-3'.

Human *LTA*-F: 5'-CATCTACTTCGTCTACTCCCAGG-3', Human *LTA*-R: 5'-CCCCGTGGTACATCGAGTG-3'.

Human *IFNG*-F: 5'-TCGGTAACTGACTTGAATGTCCA-3', Human *IFNG*-R: 5'-TCGCTTCCCTGTTTTAGCTGC-3'.

Human *GATA3*-F: 5'-GCCCCTCATTAAGCCCAAG-3', Human *GATA3*-R: 5'-TTGTGGTGGTCTGACAGTTCG-3'.

Human *CCR4*-F: 5'-AGAAGGCATCAAGGCATTTGG-3', Human *CCR4*-R: 5'-ACACATCAGTCATGGACCTGAG-3'.

Human *IL4*-F: 5'-TGAAACGGCTCGACAGGAAC-3', Human *IL4*-R: 5'-TGAATGGGTTGACCAAGGGTG-3'.

Human *IL2RA*-F: 5'-GTGGGGACTGCTCACGTTC-3', Human *IL2RA*-R: 5'-CCCGCTTTTTATTCTGCGGAA-3'.

Human *IL2RG*-F: 5'-GTGCAGCCACTATCTATTCTCTG-3', Human *IL2RG*-R: 5'-GTGAAGTGTTAGGTTCTCTGGAG-3'.

Human *TGFB1*-F: 5'-CAATTCCTGGCGATACCTCAG-3', Human *TGFB1*-R: 5'-GCACAACTCCGGTGACATCAA-3'.

Cell line derived (CDX) xenograft models

HH cells (3×10^6 each mouse) or Hut78 cells (8×10^6 each mouse) were inoculated subcutaneously into nude mice (Shanghai Laboratory of Animal Center, Chinese Academy of Sciences) or NOD.Cg-Prkdc^{scid}Il2rg^{tm1Wjl}/SzJ (NSG) mice (The Jackson Laboratory) respectively and tumor volume was monitored. Animal care and experiments were performed in strict accordance with the "Guide for the Care and Use

of Laboratory Animals" and the "Principles for the Utilization and Care of Vertebrate Animals" and were approved by the committee for humane treatment of animals at Shanghai Jiao Tong University School of Medicine.

IHC (Immunohistochemistry)

For histology, samples were fixed in 4% paraformaldehyde overnight before standard processing for paraffin-embedded tissues. Then, 10-μm sections were stained with IHC. The paraffin sections of human skin tissues and mice tumor tissues were dewaxed, antigen retrieval and blocked with 5% BSA as per standard protocols. Sections were stained using the polyclonal antibodies CDK9 (2316, Cell Signaling Technology) or CD25 (AF7224, Beyotime).

Integrated analysis of public CTCL scRNA-seq datasets

Count matrices from three studies including GSE165623 (n = 3), GSE171811 (n = 14), and GSE128531 (n = 9) were downloaded from the Gene Expression Omnibus and re-analyzed respectively. Doublets or multiple cells, and low quality barcodes (including dead or dying cells) were initially removed if having less than 200 expressed genes or more than 40% mitochondrial transcripts. Genes that were detected in fewer than 60 cells were also filtered out. Seurat (v3.0.2) anchor-based integration using canonical correlational analysis and mutual nearest neighbors was performed to eliminate the biological and technical batch effects of the samples and scRNA-seq libraries[2]. The count data were normalized by a scale factor (10,000) followed by a natural-log transformation. The top 3,000 highly variable genes (HVGs) which were detected using the "FindVariableGenes" function were subsequently used to identify the integration

anchors based on the first 30 dimensions by employing the “IntegrateData” function. Principal component analysis (PCA) was performed using the “RunPCA” function to project the cells in a two-dimensional space. A graph-based Louvain clustering and dimensional reduction to form the Uniform Manifold Approximation and Projection (UMAP) plots used the top 30 calculated dimensions following a resolution of 0.6 for GSE165623, 0.4 for GSE171811 and 0.9 for GSE128531 respectively.

Cell type labels were assigned to clusters based on the inference from scHCL package (v0.1.1)[3] and the expression of signature genes. Cell cycle state of T cells was evaluated by Seurat “CellCycleScoring” function based on a list of canonical markers delineating G1, S and G2/M phases described in Tirosh *et al*., 2016[4]. Clonotype annotation files were obtained from GSE165623 and GSE171811. Three types of T cells were assigned as follows: 1) malignant cells: cells with the highest CDR3 sequence frequency for TCR β, 2) polyclonal cells: all T cells that possess non-malignant clonotype based on the CDR3 sequence, 3) remaining cells: T cell barcodes without TCR detected.

Bulk RNA-seq data processing

For the gene expression, we mapped the sequencing data to reference genome (hg38) using HISAT, and defined transcript coordinates according to the gene annotation format file (GTF file) from GENCODE (Release 27, GRCh38). The Gene abundances are given as Reads Per Kilobase per Million mapped reads (RPKM) with “cuffnorm” command using the Cufflinks package.

MS data processing

All MS/MS ion spectra were analyzed using PEAKS X (Bioinformatics Solutions) for processing, *de novo* sequencing, database searching and label-free quantification. Resulting sequences were searched against the UniProt Human Proteome database (downloaded 5 May 2018) with mass error tolerances of 10 ppm and 0.02 Da for parent and fragment, respectively, the digestion enzyme semiTrypsin allowed for two missed tryptic cleavages, Carbamidomethyl of cysteine specified as a fixed modification, and Oxidation of methionine, acetyl of the N-terminus and phosphorylation of tyrosine, serine, and threonine as variable modifications. FDR estimation was enabled. Peptides were filtered for $-10\log P \geq 15$, and proteins were filtered for $-10\log P \geq 15$ and one unique peptide. For all experiments, this gave an FDR of <1% at the peptide-spectrum match level. Proteins sharing significant peptide evidence were grouped.

Intracellular cytokine staining

HH cells or Hut 78 cells were treated with ATRA (1 μM) or DMSO for 48 h. Thoroughly resuspend cells were fixed and permeabilized in 250 μl of BD Cytofix/Cytoperm solution (BD Biosciences, 51-2090 KZ) and incubated for 20 min at 4 °C. Wash cells two times in BD Perm/Wash buffer (BD Biosciences, 51-2091 KZ). Thoroughly resuspend fixed/permeabilized cells in 50 μl of BD Perm/Wash buffer (BD Biosciences, 51-2091 KZ) containing 0.5 μl of Foxp3 Monoclonal Antibody (Invitrogen, 12577380) or 0.5 μl of IgG Mouse-PE Isotype Control (Beckman, IM0670U). Incubate at 4 °C for 30 min in the dark. Flow cytometric data were acquired using flow cytometer (Cytoflex s, Beckman). Data were analyzed using FlowJo software.

Flow cytometry

HH cells or Hut 78 cells were treated with ATRA (2 μM) or DMSO for 48 h, followed by staining with antibodies against CD25 (Invitrogen, 25-0259-42), CD5 (Invitrogen, 12-0059-42) and CD7 (Invitrogen, 11-0078-42). The immunophenotyping was performed on flow cytometry (Cytoflex s, Beckman).

Plasmids, virus construction and infection

Information on all of the plasmids is provided in Supplementary Table 6. Information on the shRNA sequences is provided in Supplementary Table 7. Lentivirus was produced by co-transfecting 293T cells with the lentiviral construct pCMV-dR8.91 (Δ8.9) plasmid, containing the genes gag, pol and rev, and the pMDG envelope-expressing plasmid, using Lipofectamine 2000 (Invitrogen, 11668500). Viral supernatant was harvested at 48 h post-transfection, passed through a 0.45 μm filter and infected the indicated leukemia cells using polybrene (Sigma-Aldrich).

Supplementary Table 6. List of plasmids used in this study

CDS	Vector
3×Flag-CDK9	pLVX-IRES-Puro
3×Flag-CDK9-T186A	pLVX-IRES-Puro
3×Flag-CDK9-S347E	pLVX-IRES-Puro
Myc-ubiquitin	pcDNA3.1
HUWE1	pcDNA4.0
3×HA-RARα	pLVX-IRES-Puro

3×HA-RARα (ΔAF1)	pLVX-IRES-Puro
3×HA-RARα (ΔDBD)	pLVX-IRES-Puro
3×HA-RARα (ΔHinge)	pLVX-IRES-Puro
3×HA-RARα (ΔABD)	pLVX-IRES-Puro
3×HA-RARα (ΔAF2)	pLVX-IRES-Puro
3×HA-RARα-K244R	pLVX-IRES-Puro
3×HA-RARα-K360R	pLVX-IRES-Puro
3×HA-ΔH-RARα-K244R	pLVX-IRES-Puro
3×HA-ΔH-RARα-K360R	pLVX-IRES-Puro
GST-CDK9	pGEX-6P-1
GST-CDK9-T186A	pGEX-6P-1
GST-CDK9-S347E	pGEX-6P-1
GST-CDK9 (ΔG-Loop)	pGEX-6P-1
GST-CDK9 (ΔCBD)	pGEX-6P-1
GST-CDK9 (ΔCL)	pGEX-6P-1
GST-CDK9 (ΔT-Loop)	pGEX-6P-1

Supplementary Table 7. Target sequences of shRNAs used in this study

shRNA	Vector	Target sequence (5'-3')
shCDK9-1	pLKO.1-Puro	CTACTACATCCACAGAAACAA
shCDK9-2	pLKO.1-Puro	GTTCGACTTCTGCGAGCATGA
shCDK9-3	pLKO-Tet-On	GCACAGTTTGGTCCGTTAGAA

shRARα-1	pLKO.1-hygro	CCCAAGATGCTAATGAAGATT
shRARα-5	pLKO-Tet-On	GGTATTAATTCTCGCTGGTTT
shHUWE1-1	PGIPZ-GFP-puro	CACATGCTACTGTTGGCTA
shHUWE1-2	PGIPZ-GFP-puro	AGCTTCTTTACGAACATTA
shHUWE1-3	PGIPZ-GFP-puro	TGGTAGATGTCCTTCAGAT
shHUWE1-4	PGIPZ-GFP-puro	CTCAATCTCCTATATGTAT

Chemical synthesis

General methods.

Reagents and solvents were purchased from commercial sources without further purification, unless otherwise indicated. Starting materials of **S2** and **S3** are synthesized according to the patent WO2019196812. The progress of reactions was monitored by thin-layer chromatography (TLC) and/or LC-MS. The final compounds were purified by prepared HPLC. NMR spectra were obtained from an Ascend 400 MHz Bruker spectrometer (operating at 400 MHz for 1H NMR). Multiplicities of signals are described as follows: s --- singlet, br. s --- broad singlet, d --- doublet, t --- triplet, m --- multiple. High Resolution Mass spectra were recorded on Agilent-6125B ESI mass spectrometer with acetonitrile and water as solvents.

Scheme S1. Synthesis of compound **1**-**22**

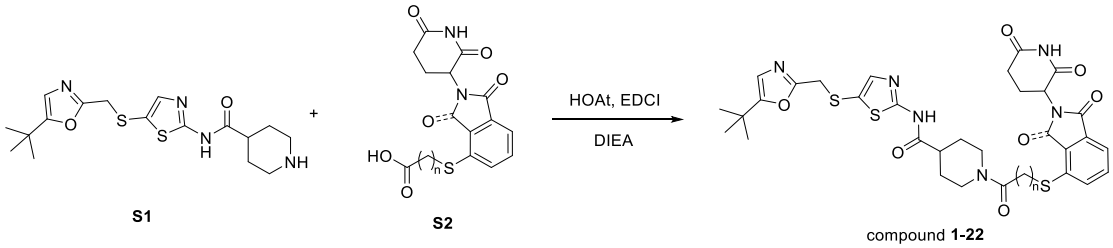

General procedure.

To a mixture of *N*-[5-({[5-(2-methylprop-2-yl)-1,3-oxazol-2-yl]methyl}sulfanyl)-1,3-thiazol-2-yl]hexahydropyridine-4-carboxamide **S1** (20 mg, 0.053 mmol), **S2** (0.053 mmol, 1.0 eq), EDCI (20.3 mg, 0.106 mmol, 2.0 eq), HOAt (14.4 mg, 0.106 mmol, 2.0 eq) and DMF (5 mL) were added DIEA (43.8 μL, 0.265 mmol, 5.0 eq). The mixture was stirred for 2 hours at room-temperature. LC-MS showed compound **S1** was consumed and the desired product was major. The mixture was purified by prep-HPLC (0.05% HCl aq./acetonitrile) and lyophilized to give the desired product.

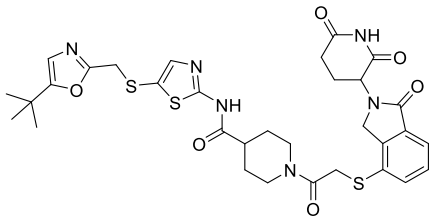

N-(5-(((5-(*tert*-butyl)oxazol-2-yl)methyl)thio)thiazol-2-yl)-1-(2-((2-(2,6-dioxopiperidin-3-yl)-1-oxoisoindolin-4-yl)thio)acetyl)piperidine-4-carboxamide (**1**). Light yellow solid (18.5 mg, yield 50%).^{1}H NMR (400 MHz, DMSO-d_6) δ 12.33 (s, 1H), 11.00 (d, J = 3.2 Hz, 1H), 7.72 (t, J = 6.1 Hz, 1H), 7.56 (dd, J = 15.8, 9.5 Hz, 2H), 7.40 (d, J = 5.4 Hz, 1H), 6.72 (s, 1H), 5.14 (dd, J = 13.3, 4.6 Hz, 1H), 4.41 – 4.30 (m, 2H), 4.21 – 4.11 (m, 2H), 4.06 (s, 2H), 4.01 (d, J = 13.3 Hz, 1H), 3.18 – 3.02 (m, 2H), 2.94 (dd, J = 22.1, 8.7 Hz, 1H), 2.80 – 2.66 (m, 2H), 2.61 (d, J = 18.3 Hz, 1H), 2.48 (s,

1H), 2.06 – 1.98 (m, 1H), 1.83 (s, 2H), 1.68 (d, J = 12.4 Hz, 1H), 1.43 (s, 1H), 1.18 (d, J = 3.1 Hz, 9H). MS (ESI) m/z: calcd. for $C_{32}H_{37}N_6O_6S_3^+$ $[M+H]^+$, 697.19; found 697.3.

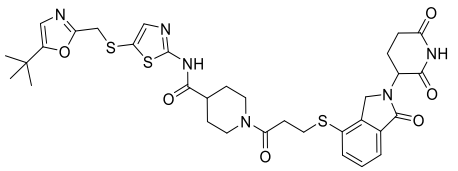

N-(5-(((5-(*tert*-butyl)oxazol-2-yl)methyl)thio)thiazol-2-yl)-1-(3-((2-(2,6-dioxopiperidin-3-yl)-1-oxoisoindolin-4-yl)thio)propanoyl)piperidine-4-carboxamide (**2**). Light yellow solid (18.8 mg, yield 52%). ^{1}H NMR (400 MHz, DMSO-d_6) δ 12.30 (s, 1H), 10.99 (s, 1H), 7.67 (d, J = 7.2 Hz, 1H), 7.60 – 7.52 (m, 2H), 7.40 (d, J = 8.0 Hz, 1H), 6.76 – 6.68 (m, 1H), 5.13 (d, J = 13.1 Hz, 1H), 4.40 – 4.33 (m, 2H), 4.23 (dd, J = 17.4, 5.8 Hz, 1H), 4.06 (s, 2H), 3.83 (s, 1H), 3.27 (d, J = 6.6 Hz, 2H), 3.00 (t, J = 11.8 Hz, 1H), 2.95 – 2.86 (m, 1H), 2.73 (dd, J = 14.2, 8.3 Hz, 3H), 2.64 – 2.57 (m, 2H), 2.46 (s, 1H), 2.07 – 1.97 (m, 1H), 1.80 (d, J = 12.7 Hz, 2H), 1.62 – 1.49 (m, 1H), 1.42 (d, J = 12.7 Hz, 1H), 1.18 (d, J = 4.6 Hz, 9H). MS (ESI) m/z: calcd. for $C_{33}H_{39}N_6O_6S_3^+$ $[M+H]^+$, 711.21; found 711.2.

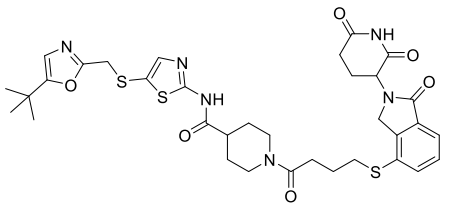

N-(5-(((5-(*tert*-butyl)oxazol-2-yl)methyl)thio)thiazol-2-yl)-1-(4-((2-(2,6-dioxopiperidin-3-yl)-1-oxoisoindolin-4-yl)thio)butanoyl)piperidine-4-carboxamide (**3**). Light yellow solid (17.7 mg, yield 46%). ^{1}H NMR (400 MHz, DMSO-d_6) δ 12.30 (s,

1H), 10.99 (s, 1H), 7.69 (dt, *J* = 11.0, 5.5 Hz, 1H), 7.58 – 7.48 (m, 2H), 7.40 (d, *J* = 7.0 Hz, 1H), 6.76 – 6.65 (m, 1H), 5.13 (dd, *J* = 13.3, 5.1 Hz, 1H), 4.30 (dd, *J* = 58.2, 17.4 Hz, 3H), 4.06 (s, 2H), 3.87 (d, *J* = 11.7 Hz, 1H), 3.15 – 3.09 (m, 2H), 3.01 (t, *J* = 12.3 Hz, 1H), 2.95 – 2.86 (m, 1H), 2.75 – 2.54 (m, 4H), 2.49 – 2.37 (m, 2H), 2.05 – 1.98 (m, 1H), 1.82 (dd, *J* = 14.1, 7.2 Hz, 4H), 1.53 (d, *J* = 12.5 Hz, 1H), 1.40 (d, *J* = 9.4 Hz, 1H), 1.18 (d, *J* = 3.6 Hz, 9H). MS (ESI) m/z: calcd. for $C_{34}H_{41}N_6O_6S_3^+$ $[M+H]^+$, 725.22; found 725.3.

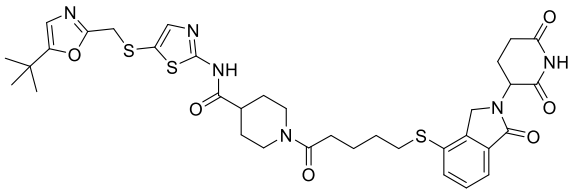

N-(5-(((5-(*tert*-butyl)oxazol-2-yl)methyl)thio)thiazol-2-yl)-1-(5-((2-(2,6-dioxopiperidin-3-yl)-1-oxoisoindolin-4-yl)thio)pentanoyl)piperidine-4-carboxamide (**4**). Light yellow solid (16.1 mg, yield 41%). ^{1}H NMR (400 MHz, DMSO-d_6) δ 12.30 (s, 1H), 10.99 (s, 1H), 7.65 (dd, *J* = 7.3, 1.3 Hz, 1H), 7.60 – 7.47 (m, 2H), 7.40 (d, *J* = 7.6 Hz, 1H), 6.72 (s, 1H), 5.13 (dd, *J* = 13.3, 5.1 Hz, 1H), 4.30 (dd, *J* = 57.6, 17.4 Hz, 3H), 4.06 (s, 2H), 3.92 (t, *J* = 14.5 Hz, 1H), 3.11 (s, 2H), 3.01 (t, *J* = 11.7 Hz, 1H), 2.98 – 2.85 (m, 1H), 2.72 (dd, *J* = 13.1, 9.5 Hz, 1H), 2.64 – 2.54 (m, 2H), 2.49 – 2.27 (m, 3H), 2.07 – 1.94 (m, 1H), 1.80 (s, 2H), 1.64 (d, *J* = 3.1 Hz, 4H), 1.54 (d, *J* = 12.1 Hz, 1H), 1.38 (dd, *J* = 23.0, 13.7 Hz, 1H), 1.18 (d, *J* = 4.8 Hz, 9H). MS (ESI) m/z: calcd. for $C_{35}H_{43}N_6O_6S_3^+$ $[M+H]^+$, 739.24; found 739.3.

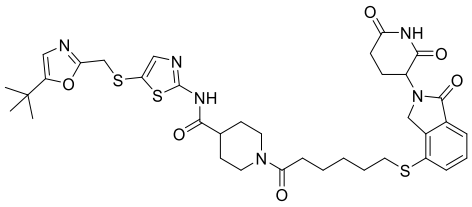

N-(5-(((5-(*tert*-butyl)oxazol-2-yl)methyl)thio)thiazol-2-yl)-1-(6-((2-(2,6-dioxopiperidin-3-yl)-1-oxoisoindolin-4-yl)thio)hexanoyl)piperidine-4-carboxamide (**5**). Light yellow solid (21.9 mg, yield 55%). ^{1}H NMR (400 MHz, DMSO-d_6) δ 12.30 (s, 1H), 10.99 (s, 1H), 7.63 (t, J = 6.7 Hz, 1H), 7.59 – 7.52 (m, 2H), 7.41 (d, J = 7.1 Hz, 1H), 6.76 – 6.68 (m, 1H), 5.13 (dd, J = 13.3, 5.1 Hz, 1H), 4.40 – 4.19 (m, 3H), 4.06 (s, 2H), 3.89 (d, J = 13.2 Hz, 1H), 3.09 (t, J = 7.2 Hz, 2H), 3.00 (d, J = 11.4 Hz, 1H), 2.96 – 2.87 (m, 1H), 2.72 (t, J = 11.5 Hz, 1H), 2.64 – 2.55 (m, 2H), 2.49 – 2.40 (m, 1H), 2.32 – 2.26 (m, 2H), 2.04 – 1.98 (m, 1H), 1.80 (s, 2H), 1.61 (dd, J = 13.9, 7.1 Hz, 2H), 1.56 – 1.48 (m, 3H), 1.46 – 1.37 (m, 3H), 1.18 (d, J = 4.5 Hz, 9H). MS (ESI) m/z: calcd. for $C_{36}H_{45}N_6O_6S_3^+$ $[M+H]^+$, 753.26; found 753.3.

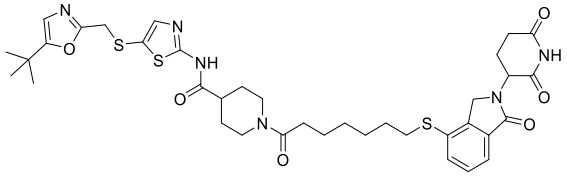

N-(5-(((5-(*tert*-butyl)oxazol-2-yl)methyl)thio)thiazol-2-yl)-1-(7-((2-(2,6-dioxopiperidin-3-yl)-1-oxoisoindolin-4-yl)thio)heptanoyl)piperidine-4- carboxamide (**6**). Light yellow solid (18.3 mg, yield 45%). ^{1}H NMR (400 MHz, DMSO-d_6) δ 12.31 (s, 1H), 10.99 (s, 1H), 7.63 (dt, J = 6.6, 3.3 Hz, 1H), 7.59 – 7.52 (m, 2H), 7.40 (d, J = 6.9 Hz, 1H), 6.72 (d, J = 3.5 Hz, 1H), 5.13 (dd, J = 13.3, 5.1 Hz, 1H), 4.39 – 4.19 (m, 3H), 4.06 (s, 2H), 3.89 (d, J = 13.7 Hz, 1H), 3.09 (t, J = 7.2 Hz, 2H), 3.00 (d, J = 12.5

Hz, 1H), 2.94 – 2.86 (m, 1H), 2.73 (t, J = 11.5 Hz, 1H), 2.63 – 2.54 (m, 2H), 2.49 – 2.42 (m, 1H), 2.32 – 2.25 (m, 2H), 2.05 – 1.97 (m, 1H), 1.80 (s, 2H), 1.60 (dd, J = 14.3, 7.2 Hz, 2H), 1.46 (ddd, J = 21.9, 14.5, 7.3 Hz, 6H), 1.33 – 1.27 (m, 2H), 1.18 (d, J = 4.6 Hz, 9H). MS (ESI) m/z: calcd. for $C_{37}H_{47}N_6O_6S_3^+$ $[M+H]^+$, 767.27; found 767.3.

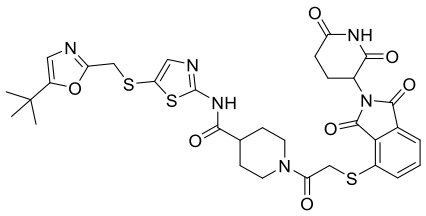

N-(5-(((5-(*tert*-butyl)oxazol-2-yl)methyl)thio)thiazol-2-yl)-1-(2-((2-(2,6-dioxopiperidin-3-yl)-1,3-dioxoisoindolin-4-yl)thio)acetyl)piperidine-4-carboxamide (**7**). Yellow solid (13.9 mg, 37%). ^{1}H NMR (400 MHz, DMSO-d_6) δ 12.31 (s, 1H), 10.99 (s, 1H), 7.63 (dt, J = 6.6, 3.3 Hz, 1H), 7.59 – 7.52 (m, 2H), 7.40 (d, J = 6.9 Hz, 1H), 6.72 (d, J = 3.5 Hz, 1H), 5.13 (dd, J = 13.3, 5.1 Hz, 1H), 4.39 – 4.19 (m, 3H), 4.06 (s, 2H), 3.89 (d, J = 13.7 Hz, 1H), 3.09 (t, J = 7.2 Hz, 2H), 3.00 (d, J = 12.5 Hz, 1H), 2.94 – 2.86 (m, 1H), 2.73 (t, J = 11.5 Hz, 1H), 2.63 – 2.54 (m, 2H), 2.49 – 2.42 (m, 1H), 2.32 – 2.25 (m, 2H), 2.05 – 1.97 (m, 1H), 1.80 (s, 2H), 1.60 (dd, J = 14.3, 7.2 Hz, 2H), 1.46 (ddd, J = 21.9, 14.5, 7.3 Hz, 6H), 1.33 – 1.27 (m, 2H), 1.18 (d, J = 4.6 Hz, 9H). MS (ESI) m/z: calcd. for $C_{32}H_{35}N_6O_7S_3$+ $[M+H]^+$, 711.17; found 711.2.

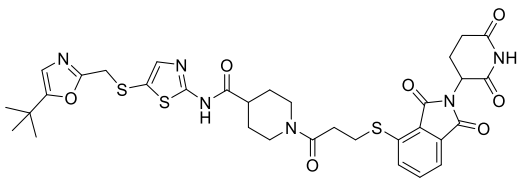

N-(5-(((5-(*tert*-butyl)oxazol-2-yl)methyl)thio)thiazol-2-yl)-1-(3-((2-(2,6-dioxopiperidin-3-yl)-1,3-dioxoisoindolin-4-yl)thio)propanoyl)piperidine-4-carboxamide (**8**). Yellow solid (15.4 mg, 40%). ^{1}H NMR (400 MHz, DMSO-d_6) δ 12.36 (d, J = 47.6 Hz, 1H), 11.12 (s, 1H), 7.86 – 7.74 (m, 2H), 7.68 – 7.59 (m, 1H), 7.40 (d, J = 7.5 Hz, 1H), 6.76 – 6.65 (m, 1H), 5.12 (dd, J = 12.8, 5.4 Hz, 1H), 4.40 (d, J = 13.4 Hz, 1H), 4.10 – 4.02 (m, 2H), 3.88 (d, J = 14.3 Hz, 1H), 3.03 (t, J = 12.9 Hz, 1H), 2.93 – 2.52 (m, 9H), 2.07 (dd, J = 12.4, 7.0 Hz, 1H), 1.81 (d, J = 11.5 Hz, 2H), 1.64 – 1.48 (m, 1H), 1.43 (d, J = 12.6 Hz, 1H), 1.23 – 1.16 (m, 9H). MS (ESI) m/z: calcd. for $C_{33}H_{37}N_6O_7S_3^+$ $[M+H]^+$, 725.19; found 725.2.

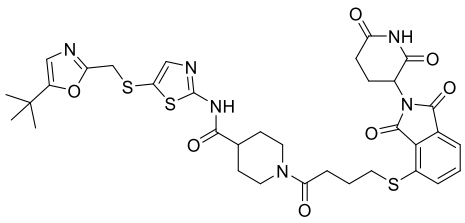

N-(5-(((5-(*tert*-butyl)oxazol-2-yl)methyl)thio)thiazol-2-yl)-1-(4-((2-(2,6-dioxopiperidin-3-yl)-1,3-dioxoisoindolin-4-yl)thio)butanoyl)piperidine-4-carboxamide (**9**). Yellow solid (19.2 mg, 49%). ^{1}H NMR (400 MHz, DMSO-d_6) δ 12.31 (s, 1H), 11.13 (s, 1H), 7.88 (d, J = 8.2 Hz, 1H), 7.84 – 7.76 (m, 1H), 7.64 (d, J = 7.1 Hz, 1H), 7.40 (s, 1H), 6.73 (d, J = 4.9 Hz, 1H), 5.12 (dd, J = 12.8, 5.4 Hz, 1H), 4.41 (d, J = 12.7 Hz, 1H), 4.06 (s, 2H), 3.91 (d, J = 12.9 Hz, 1H), 3.19 – 3.13 (m, 2H), 3.05 (t, J = 11.8 Hz, 1H), 2.89 (td, J = 13.5, 6.4 Hz, 1H), 2.74 (t, J = 11.2 Hz, 1H), 2.68 – 2.52

(m, 5H), 2.11 – 2.02 (m, 1H), 1.92 – 1.77 (m, 4H), 1.63 – 1.51 (m, 1H), 1.48 – 1.37 (m, 1H), 1.18 (s, 9H). MS (ESI) m/z: calcd. for $C_{34}H_{39}N_6O_7S_3^+$ $[M+H]^+$, 739.20; found 739.3.

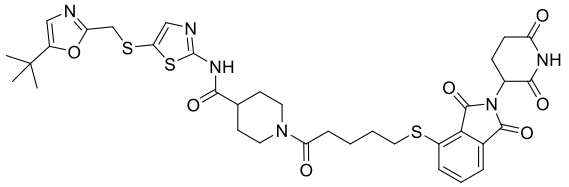

N-(5-(((5-(*tert*-butyl)oxazol-2-yl)methyl)thio)thiazol-2-yl)-1-(5-((2-(2,6-dioxopiperidin-3-yl)-1,3-dioxoisoindolin-4-yl)thio)pentanoyl)piperidine-4-carboxamide (**10**). Yellow solid (21.5 mg, 54%). ^{1}H NMR (400 MHz, DMSO-d_6) δ 12.30 (s, 1H), 11.13 (s, 1H), 7.88 – 7.72 (m, 2H), 7.62 (t, J = 11.8 Hz, 1H), 7.40 (d, J = 7.1 Hz, 1H), 6.81 – 6.66 (m, 1H), 5.12 (dd, J = 12.7, 5.4 Hz, 1H), 4.39 (d, J = 12.7 Hz, 1H), 4.04 (d, J = 14.3 Hz, 2H), 3.93 (d, J = 13.1 Hz, 1H), 3.16 (d, J = 6.4 Hz, 2H), 3.03 (t, J = 12.2 Hz, 1H), 2.93 – 2.84 (m, 1H), 2.72 (d, J = 11.2 Hz, 1H), 2.66 – 2.53 (m, 3H), 2.39 (d, J = 5.0 Hz, 2H), 2.07 (dd, J = 12.1, 6.8 Hz, 1H), 1.81 (s, 2H), 1.69 (d, J = 6.0 Hz, 4H), 1.55 (d, J = 9.2 Hz, 1H), 1.44 – 1.31 (m, 1H), 1.18 (d, J = 4.4 Hz, 9H). MS (ESI) m/z: calcd. for $C_{35}H_{41}N_6O_7S_3^+$ $[M+H]^+$, 753.22; found 753.3.

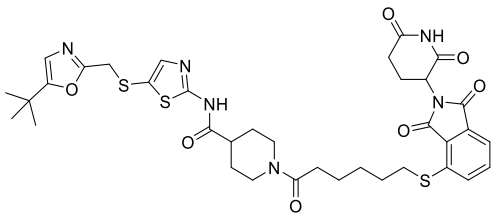

N-(5-(((5-(*tert*-butyl)oxazol-2-yl)methyl)thio)thiazol-2-yl)-1-(6-((2-(2,6-dioxopiperidin-3-yl)-1,3-dioxoisoindolin-4-yl)thio)hexanoyl)piperidine-4-

carboxamide (**11**). Yellow solid (19.5 mg, 48%).^{1}H NMR (400 MHz, DMSO-d_6) δ 12.30 (s, 1H), 11.12 (s, 1H), 7.85 – 7.71 (m, 2H), 7.62 (t, J = 8.8 Hz, 1H), 7.40 (d, J = 6.6 Hz, 1H), 6.79 – 6.66 (m, 1H), 5.12 (dd, J = 12.7, 5.4 Hz, 1H), 4.39 (d, J = 13.5 Hz, 1H), 4.05 (d, J = 6.0 Hz, 2H), 3.92 (d, J = 13.7 Hz, 1H), 3.14 (t, J = 7.2 Hz, 2H), 3.03 (t, J = 12.4 Hz, 1H), 2.94 – 2.84 (m, 1H), 2.73 (t, J = 11.2 Hz, 1H), 2.65 – 2.52 (m, 3H), 2.37 – 2.28 (m, 2H), 2.06 (dd, J = 12.4, 6.9 Hz, 1H), 1.81 (s, 2H), 1.73 – 1.65 (m, 2H), 1.60 – 1.36 (m, 6H), 1.24 – 1.16 (m, 9H). MS (ESI) m/z: calcd. for $C_{36}H_{43}N_6O_7S_3^+$ $[M+H]^+$, 767.23; found 767.3.

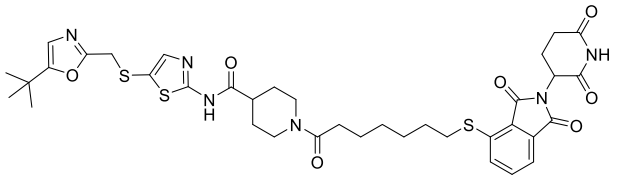

N-(5-(((5-(*tert*-butyl)oxazol-2-yl)methyl)thio)thiazol-2-yl)-1-(7-((2-(2,6-dioxopiperidin-3-yl)-1,3-dioxoisoindolin-4-yl)thio)heptanoyl)piperidine-4-carboxamide (**12**). Yellow solid (17.8 mg, 43%).^{1}H NMR (400 MHz, DMSO-d_6) δ 12.30 (s, 1H), 11.12 (s, 1H), 7.85 – 7.71 (m, 2H), 7.67 – 7.57 (m, 1H), 7.40 (d, J = 7.0 Hz, 1H), 6.77 – 6.66 (m, 1H), 5.12 (dd, J = 12.8, 5.4 Hz, 1H), 4.39 (d, J = 12.2 Hz, 1H), 4.05 (s, 2H), 3.91 (d, J = 13.7 Hz, 1H), 3.13 (t, J = 7.3 Hz, 2H), 3.03 (t, J = 12.0 Hz, 1H), 2.95 – 2.82 (m, 1H), 2.72 (dd, J = 21.2, 10.0 Hz, 1H), 2.57 (dd, J = 25.4, 13.1 Hz, 3H), 2.38 – 2.26 (m, 2H), 2.06 (dd, J = 10.7, 5.4 Hz, 1H), 1.81 (s, 2H), 1.67 (dd, J = 14.3, 7.2 Hz, 2H), 1.56 – 1.30 (m, 8H), 1.23 – 1.14 (m, 9H). MS (ESI) m/z: calcd. for $C_{37}H_{45}N_6O_7S_3^+$ $[M+H]^+$, 781.25; found 781.3.

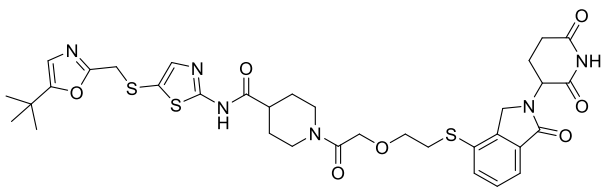

N-(5-(((5-(*tert*-butyl)oxazol-2-yl)methyl)thio)thiazol-2-yl)-1-(2-(2-((2-(2,6-dioxopiperidin-3-yl)-1-oxoisoindolin-4-yl)thio)ethoxy)acetyl)piperidine-4-carboxamide (**13**). Light yellow solid (17.7 mg, 45%). ^{1}H NMR (400 MHz, DMSO-d$_6$) δ 12.31 (s, 1H), 10.99 (s, 1H), 7.69 (s, 1H), 7.60 – 7.54 (m, 2H), 7.40 (t, *J* = 3.3 Hz, 1H), 6.72 (d, *J* = 4.5 Hz, 1H), 5.13 (dd, *J* = 13.1, 5.0 Hz, 1H), 4.44 – 4.22 (m, 3H), 4.18 (d, *J* = 15.7 Hz, 1H), 4.05 (d, *J* = 6.8 Hz, 2H), 3.77 (s, 1H), 3.68 (d, *J* = 6.0 Hz, 2H), 3.28 (s, 2H), 3.03 – 2.96 (m, 1H), 2.93 – 2.87 (m, 1H), 2.73 (s, 1H), 2.68 – 2.53 (m, 3H), 2.49 – 2.42 (m, 1H), 2.01 (d, *J* = 11.8 Hz, 1H), 1.80 (d, *J* = 12.0 Hz, 2H), 1.60 (s, 1H), 1.46 – 1.32 (m, 1H), 1.18 (d, *J* = 6.2 Hz, 9H). MS (ESI) m/z: calcd. for $C_{34}H_{41}N_6O_7S_3^+$ $[M+H]^+$, 741.22; found 741.3.

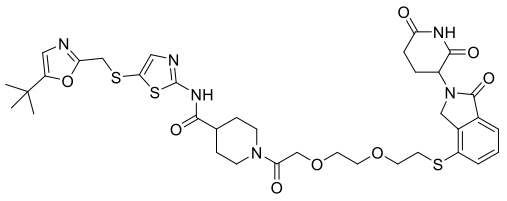

N-(5-(((5-(*tert*-butyl)oxazol-2-yl)methyl)thio)thiazol-2-yl)-1-(2-(2-(2-((2-(2,6-dioxopiperidin-3-yl)-1-oxoisoindolin-4-yl)thio)ethoxy)ethoxy)acetyl)piperidine-4-carboxamide (**14**). Light yellow solid (19.6 mg, 47%). ^{1}H NMR (400 MHz, DMSO-*d*$_6$) δ 12.23 (s, 1H), 10.92 (s, 1H), 7.62 (d, *J* = 7.5 Hz, 1H), 7.54 – 7.40 (m, 2H), 7.33 (d, *J* = 8.4 Hz, 1H), 6.65 (d, *J* = 5.1 Hz, 1H), 5.06 (dd, *J* = 13.2, 5.0 Hz, 1H), 4.35 – 4.13 (m, 3H), 4.06 (d, *J* = 19.6 Hz, 1H), 3.98 (s, 2H), 3.75 (d, *J* = 11.9 Hz, 1H), 3.56 (t, *J* = 6.4

Hz, 2H), 3.47 (s, 4H), 3.19 (t, J = 6.4 Hz, 2H), 2.97 – 2.88 (m, 1H), 2.82 (dd, J = 17.5, 5.5 Hz, 1H), 2.64 (d, J = 11.3 Hz, 1H), 2.59 – 2.45 (m, 3H), 2.40 – 2.30 (m, 1H), 1.98 – 1.89 (m, 1H), 1.73 (d, J = 11.5 Hz, 2H), 1.52 (d, J = 11.2 Hz, 1H), 1.35 (d, J = 9.8 Hz, 1H), 1.11 (d, J = 5.7 Hz, 9H). MS (ESI) m/z: calcd. for $C_{36}H_{45}N_6O_8S_3^+$ $[M+H]^+$, 785.25; found 785.3.

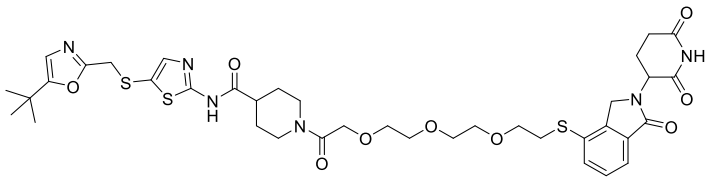

N-(5-(((5-(*tert*-butyl)oxazol-2-yl)methyl)thio)thiazol-2-yl)-1-(2-(2-(2-(2-((2-(2,6-dioxopiperidin-3-yl)-1-oxoisoindolin-4-yl)thio)ethoxy)ethoxy)ethoxy)acetyl)piperidine-4-carboxamide (**15**). Light yellow solid (18.0 mg, 41%). ^{1}H NMR (400 MHz, DMSO-d_6) δ 12.23 (s, 1H), 10.92 (s, 1H), 7.61 (d, J = 7.4 Hz, 1H), 7.53 – 7.39 (m, 2H), 7.33 (d, J = 8.7 Hz, 1H), 6.65 (d, J = 4.8 Hz, 1H), 5.06 (dd, J = 13.3, 5.0 Hz, 1H), 4.24 (dt, J = 34.4, 17.5 Hz, 3H), 4.07 (d, J = 20.2 Hz, 1H), 3.96 (d, J = 14.9 Hz, 2H), 3.76 (d, J = 12.4 Hz, 1H), 3.55 (t, J = 6.4 Hz, 2H), 3.51 – 3.42 (m, 8H), 3.17 (d, J = 6.4 Hz, 2H), 2.91 (d, J = 14.8 Hz, 1H), 2.85 – 2.77 (m, 1H), 2.64 (d, J = 11.6 Hz, 1H), 2.62 – 2.45 (m, 3H), 2.37 (d, J = 13.4 Hz, 1H), 1.98 – 1.89 (m, 1H), 1.73 (d, J = 11.6 Hz, 2H), 1.51 (d, J = 11.2 Hz, 1H), 1.34 (d, J = 13.0 Hz, 1H), 1.11 (d, J = 5.2 Hz, 9H). MS (ESI) m/z: calcd. for $C_{38}H_{49}N_6O_9S_3^+$ $[M+H]^+$, 829.27; found 829.3.

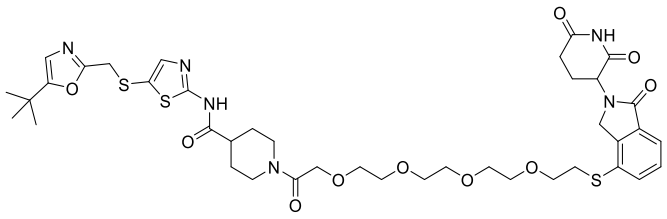

N-(5-(((5-(*tert*-butyl)oxazol-2-yl)methyl)thio)thiazol-2-yl)-1-(14-((2-(2,6-dioxopiperidin-3-yl)-1-oxoisoindolin-4-yl)thio)-3,6,9,12-tetraoxatetradecanoyl)piperidine-4-carboxamide (**16**). Light yellow solid (16.2 mg, 35%). ^{1}H NMR (400 MHz, DMSO-d_6) δ 12.23 (s, 1H), 10.92 (s, 1H), 7.61 (d, J = 7.6 Hz, 1H), 7.54 – 7.43 (m, 2H), 7.33 (d, J = 8.3 Hz, 1H), 6.64 (d, J = 4.3 Hz, 1H), 5.06 (dd, J = 13.2, 5.1 Hz, 1H), 4.36 – 4.14 (m, 3H), 4.12 – 4.00 (m, 2H), 3.98 (d, J = 4.7 Hz, 2H), 3.48 – 3.36 (m, 16H), 3.18 (t, J = 6.0 Hz, 2H), 2.87 – 2.79 (m, 1H), 2.66 (t, J = 11.1 Hz, 1H), 2.57 – 2.46 (m, 2H), 2.42 – 2.31 (m, 1H), 1.97 – 1.90 (m, 1H), 1.74 (d, J = 10.5 Hz, 2H), 1.51 (d, J = 9.5 Hz, 1H), 1.36 (d, J = 11.9 Hz, 1H), 1.11 (d, J = 4.7 Hz, 9H). MS (ESI) m/z: calcd. for $C_{40}H_{53}N_6O_{10}S_3^+$ $[M+H]^+$, 873.30; found 873.3.

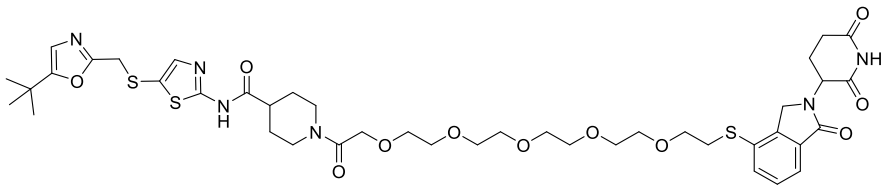

N-(5-(((5-(*tert*-butyl)oxazol-2-yl)methyl)thio)thiazol-2-yl)-1-(17-((2-(2,6-dioxopiperidin-3-yl)-1-oxoisoindolin-4-yl)thio)-3,6,9,12,15-pentaoxaheptadecanoyl)piperidine-4-carboxamide (**17**). Light yellow solid (22.4 mg, 46%). ^{1}H NMR (400 MHz, DMSO-d_6) δ 12.23 (s, 1H), 10.92 (s, 1H), 7.61 (d, J = 7.4 Hz, 1H), 7.48 (dt, J = 15.1, 7.4 Hz, 2H), 6.65 (d, J = 4.0 Hz, 1H), 5.06 (dd, J = 13.3, 5.1 Hz, 1H), 4.36 – 4.13 (m, 3H), 4.12 – 4.00 (m, 2H), 3.99 – 3.95 (m, 2H), 3.76 (d, J

= 14.2 Hz, 1H), 3.59 – 3.44 (m, 18H), 3.17 (d, *J* = 6.3 Hz, 2H), 2.90 – 2.79 (m, 2H), 2.66 (t, *J* = 11.3 Hz, 1H), 2.53 (d, *J* = 20.1 Hz, 2H), 2.38 (dd, *J* = 13.4, 9.0 Hz, 1H), 1.97 – 1.91 (m, 1H), 1.74 (d, *J* = 10.6 Hz, 2H), 1.51 (d, *J* = 9.5 Hz, 1H), 1.35 (d, *J* = 9.0 Hz, 1H), 1.11 (d, *J* = 4.5 Hz, 9H). MS (ESI) m/z: calcd. for $C_{42}H_{57}N_6O_{11}S_3^+$ $[M+H]^+$, 917.32; found 917.4.

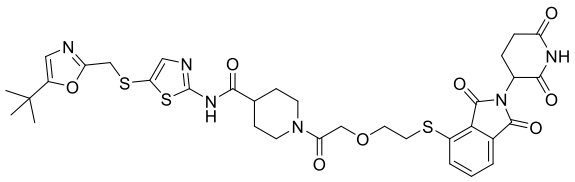

N-(5-(((5-(*tert*-butyl)oxazol-2-yl)methyl)thio)thiazol-2-yl)-1-(2-(2-((2-(2,6-dioxopiperidin-3-yl)-1,3-dioxoisoindolin-4-yl)thio)ethoxy)acetyl)piperidine-4-carboxamide (**18**). Yellow solid (16.8 mg, 42%). ^{1}H NMR (400 MHz, DMSO-d_6) δ 12.30 (s, 1H), 11.12 (s, 1H), 7.89 – 7.74 (m, 2H), 7.64 (d, *J* = 6.7 Hz, 1H), 7.39 (s, 1H), 6.75 – 6.67 (m, 1H), 5.12 (dd, *J* = 12.8, 5.3 Hz, 1H), 4.34 (s, 1H), 4.23 (d, *J* = 8.0 Hz, 2H), 4.07 (d, *J* = 10.5 Hz, 4H), 3.39 (dd, *J* = 7.4, 3.6 Hz, 4H), 2.86 (s, 1H), 2.73 (s, 1H), 2.65 – 2.54 (m, 3H), 2.07 – 1.99 (m, 1H), 1.81 (d, *J* = 10.0 Hz, 2H), 1.60 (s, 1H), 1.43 (s, 1H), 1.23 – 1.10 (m, 9H). MS (ESI) m/z: calcd. for $C_{34}H_{39}N_6O_8S_3^+$ $[M+H]^+$, 755.20; found 755.3.

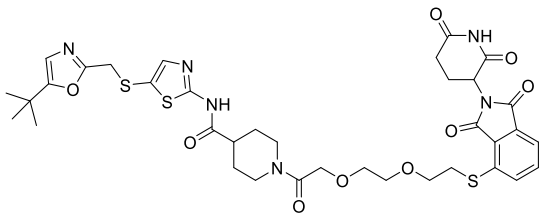

N-(5-(((5-(*tert*-butyl)oxazol-2-yl)methyl)thio)thiazol-2-yl)-1-(2-(2-(2-((2-(2,6-

dioxopiperidin-3-yl)-1,3-dioxoisoindolin-4-yl)thio)ethoxy)ethoxy)acetyl)piperidine-4-carboxamide (**19**, **GT-02865**). Yellow solid (18.6 mg, 44%). ^{1}H NMR (400 MHz, DMSO-d_6) δ 12.29 (s, 1H), 11.12 (s, 1H), 7.85 – 7.68 (m, 2H), 7.68 – 7.54 (m, 1H), 7.40 (d, J = 11.1 Hz, 1H), 6.72 (d, J = 5.0 Hz, 1H), 5.12 (dd, J = 12.7, 5.3 Hz, 1H), 4.33 (d, J = 11.9 Hz, 1H), 4.23 – 4.09 (m, 2H), 4.04 (d, J = 11.0 Hz, 2H), 3.84 (d, J = 13.3 Hz, 1H), 3.73 (t, J = 6.2 Hz, 2H), 3.64 – 3.45 (m, 6H), 2.99 (d, J = 12.8 Hz, 1H), 2.87 (d, J = 13.9 Hz, 1H), 2.73 (s, 1H), 2.60 (dd, J = 35.6, 16.8 Hz, 3H), 2.05 (d, J = 12.5 Hz, 1H), 1.81 (d, J = 12.0 Hz, 2H), 1.60 (d, J = 12.3 Hz, 1H), 1.43 (d, J = 9.8 Hz, 1H), 1.18 (d, J = 6.0 Hz, 9H). MS (ESI) m/z: calcd. for $C_{36}H_{43}N_6O_9S_3^+$ $[M+H]^+$, 799.22; found 799.3.

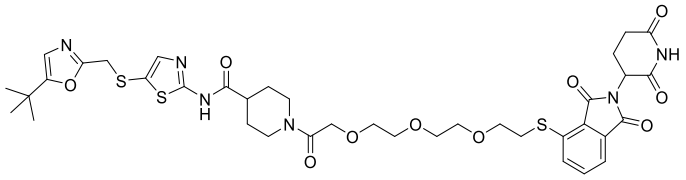

N-(5-(((5-(*tert*-butyl)oxazol-2-yl)methyl)thio)thiazol-2-yl)-1-(2-(2-(2-(2-((2-(2,6-dioxopiperidin-3-yl)-1,3-dioxoisoindolin-4-yl)thio)ethoxy)ethoxy)ethoxy)acetyl)piperidine-4-carboxamide (**20**). Yellow solid (22.8 mg, 51%). ^{1}H NMR (400 MHz, DMSO-d_6) δ 12.29 (d, J = 48.1 Hz, 1H), 11.05 (s, 1H), 7.81 – 7.66 (m, 2H), 7.56 (ddd, J = 5.9, 3.9, 2.2 Hz, 1H), 7.32 (d, J = 9.8 Hz, 1H), 6.72 – 6.59 (m, 1H), 5.05 (dd, J = 12.6, 5.3 Hz, 1H), 4.22 – 4.01 (m, 2H), 3.97 (dd, J = 12.0, 3.8 Hz, 2H), 3.75 (s, 1H), 3.64 (t, J = 6.1 Hz, 2H), 3.52 – 3.45 (m, 10H), 2.93 – 2.78 (m, 3H), 2.73 – 2.64 (m, 1H), 2.50 (dd, J = 23.7, 11.3 Hz, 3H), 1.99 (dd, J = 12.5, 6.9 Hz, 1H), 1.90 (d, J = 13.8 Hz, 1H), 1.67 (t, J = 43.3 Hz, 3H), 1.09 (t, J = 13.3 Hz,

9H). MS (ESI) m/z: calcd. for $C_{38}H_{47}N_6O_{10}S_3^+$ [M+H]$^+$, 843.25; found 843.3.

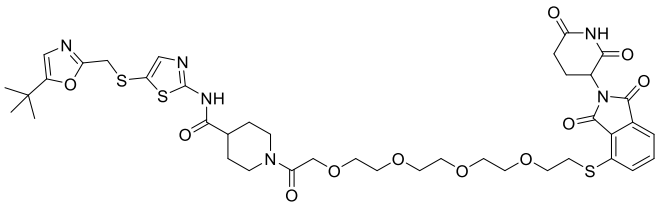

N-(5-(((5-(*tert*-butyl)oxazol-2-yl)methyl)thio)thiazol-2-yl)-1-(14-((2-(2,6-dioxopiperidin-3-yl)-1,3-dioxoisoindolin-4-yl)thio)-3,6,9,12-tetraoxatetradecanoyl)piperidine-4-carboxamide (**21**). Yellow solid (25.4 mg, 54%). ^{1}H NMR (400 MHz, DMSO-d_6) δ 12.22 (s, 1H), 11.05 (s, 1H), 7.77 – 7.66 (m, 2H), 7.56 (dd, J = 5.7, 2.2 Hz, 1H), 7.37 – 7.25 (m, 1H), 6.65 (d, J = 4.4 Hz, 1H), 5.05 (dd, J = 12.7, 5.4 Hz, 1H), 4.24 (d, J = 13.0 Hz, 1H), 4.07 (q, J = 13.6 Hz, 2H), 4.01 – 3.94 (m, 2H), 3.77 (d, J = 12.5 Hz, 1H), 3.64 (t, J = 6.3 Hz, 2H), 3.52 – 3.39 (m, 14H), 2.93 (t, J = 11.5 Hz, 1H), 2.87 – 2.78 (m, 1H), 2.64 (d, J = 12.5 Hz, 1H), 2.61 – 2.47 (m, 3H), 2.02 – 1.93 (m, 1H), 1.74 (d, J = 10.1 Hz, 2H), 1.51 (d, J = 11.8 Hz, 1H), 1.35 (d, J = 11.8 Hz, 1H), 1.16 – 1.05 (m, 9H). MS (ESI) m/z: calcd. for $C_{40}H_{51}N_6O_{11}S_3^+$ [M+H]$^+$, 887.28; found 887.3.

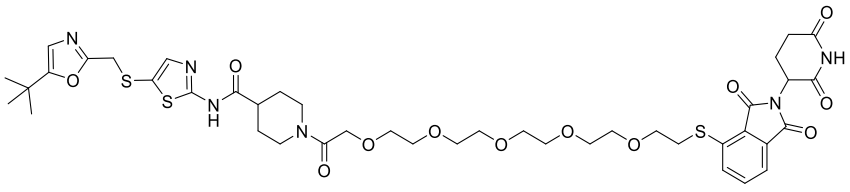

N-(5-(((5-(*tert*-butyl)oxazol-2-yl)methyl)thio)thiazol-2-yl)-1-(17-((2-(2,6-dioxopiperidin-3-yl)-1,3-dioxoisoindolin-4-yl)thio)-3,6,9,12,15-pentaoxaheptadecanoyl)piperidine-4-carboxamide (**22**). Yellow solid (19.2 mg, 39%).

^{1}H NMR (400 MHz, DMSO-d_6) δ 12.23 (s, 1H), 11.05 (s, 1H), 7.71 (dd, J = 9.0, 5.1 Hz, 2H), 7.56 (dd, J = 5.8, 2.0 Hz, 1H), 7.33 (d, J = 8.6 Hz, 1H), 6.64 (s, 1H), 5.05 (dd, J = 12.8, 5.4 Hz, 1H), 4.24 (d, J = 11.9 Hz, 1H), 4.07 (q, J = 13.6 Hz, 2H), 3.96 (d, J = 14.2 Hz, 2H), 3.76 (d, J = 14.0 Hz, 1H), 3.64 (t, J = 6.3 Hz, 2H), 3.54 – 3.41 (m, 18H), 2.98 – 2.88 (m, 1H), 2.80 (d, J = 12.1 Hz, 1H), 2.66 (s, 1H), 2.61 – 2.47 (m, 3H), 2.01 – 1.93 (m, 1H), 1.74 (d, J = 11.8 Hz, 2H), 1.52 (s, 1H), 1.35 (d, J = 9.7 Hz, 1H), 1.16 – 1.03 (m, 9H). MS (ESI) m/z: calcd. for $C_{42}H_{55}N_6O_{12}S_3^+$ $[M+H]^+$, 931.30; found 931.3.

Scheme 2: Synthesis of compound **23**-**27**

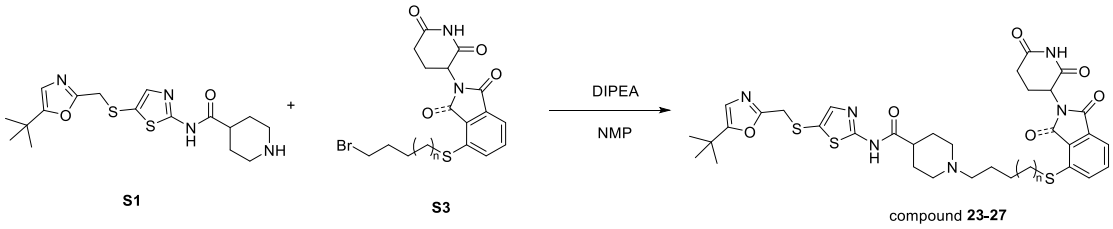

General procedure

To a solution of N-(5-(((5-(tert-butyl)oxazol-2-yl)methyl)thio)thiazol-2-yl)piperidine-4-carboxamide **S1** (26.6 mg, 0.07 mmol, 1.0 eq) in NMP (2 mL) were added bromide **S3** (0.070 mmol, 1.0 eq) and DIPEA (0.210 mmol, 3.0 eq), and the reaction was stirred at 50℃ overnight. LC-MS showed the reaction was completed. The reaction mixture was purified by prep-HPLC (0.05% HCl aq./acetonitrile) and lyophilized to afford the desired product.

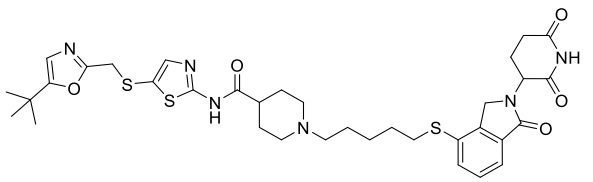

N-(5-(((5-(*tert*-butyl)oxazol-2-yl)methyl)thio)thiazol-2-yl)-1-(5-((2-(2,6-dioxopiperidin-3-yl)-1-oxoisoindolin-4-yl)thio)pentyl)piperidine-4-carboxamide (**23**, **GT-02897**). Light yellow solid (29.9 mg, 59%). ^{1}H NMR (400 MHz, DMSO-d_6) δ 12.43 (s, 1H), 11.01 (s, 1H), 9.80 (s, 1H), 7.66 (d, J = 7.4 Hz, 1H), 7.57 (dt, J = 14.7, 7.2 Hz, 2H), 7.41 (d, J = 3.7 Hz, 1H), 6.73 (s, 1H), 5.15 (dd, J = 13.3, 5.1 Hz, 1H), 4.30 (dd, J = 57.5, 17.4 Hz, 2H), 4.02 (d, J = 37.5 Hz, 2H), 3.52 (t, J = 14.5 Hz, 2H), 3.12 (t, J = 7.0 Hz, 2H), 2.99 (d, J = 16.8 Hz, 2H), 2.97 – 2.81 (m, 3H), 2.72 (dd, J = 23.9, 12.1 Hz, 1H), 2.60 (d, J = 17.2 Hz, 1H), 2.45 (dd, J = 13.1, 8.7 Hz, 1H), 2.03 (d, J = 12.6 Hz, 3H), 1.90 (dd, J = 23.6, 12.4 Hz, 2H), 1.74 – 1.56 (m, 4H), 1.45 (d, J = 7.0 Hz, 2H), 1.21 (d, J = 17.7 Hz, 9H). MS (ESI) m/z: calcd. for $C_{35}H_{45}N_6O_5S_3^+$ $[M+H]^+$, 725.26; found 725.3.

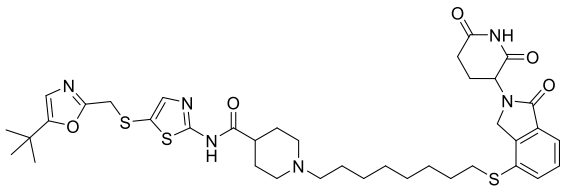

N-(5-(((5-(*tert*-butyl)oxazol-2-yl)methyl)thio)thiazol-2-yl)-1-(8-((2-(2,6-dioxopiperidin-3-yl)-1-oxoisoindolin-4-yl)thio)octyl)piperidine-4-carboxamide (**24**). Light yellow solid (32.2 mg, 0.042 mmol, 60%). ^{1}H NMR (400 MHz, DMSO-d_6) δ 12.44 (s, 1H), 11.00 (s, 1H), 9.93 (s, 1H), 7.64 (d, J = 7.3 Hz, 1H), 7.56 (dt, J = 14.8, 6.8 Hz, 2H), 7.41 (d, J = 3.4 Hz, 1H), 6.73 (d, J = 2.5 Hz, 1H), 5.14 (dd, J = 13.2, 5.0

Hz, 1H), 4.40 – 4.19 (m, 2H), 4.07 (s, 2H), 3.53 (d, *J* = 12.0 Hz, 2H), 3.09 (t, *J* = 6.8 Hz, 2H), 2.99 (dd, *J* = 10.5, 5.0 Hz, 2H), 2.95 – 2.83 (m, 3H), 2.74 (t, *J* = 12.0 Hz, 1H), 2.60 (d, *J* = 17.5 Hz, 1H), 2.45 (dd, *J* = 13.3, 8.8 Hz, 1H), 2.02 (d, *J* = 12.5 Hz, 3H), 1.98 – 1.81 (m, 2H), 1.62 (dt, *J* = 14.1, 5.9 Hz, 4H), 1.41 (s, 2H), 1.28 (s, 6H), 1.19 (s, 9H). MS (ESI) m/z: calcd. for $C_{38}H_{51}N_6O_5S_3^+$ $[M+H]^+$, 767.31; found 767.3.

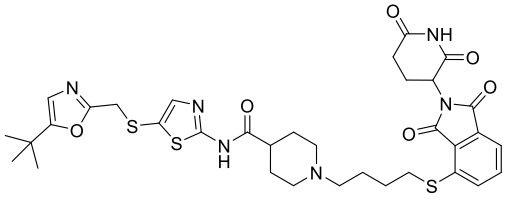

N-(5-(((5-(*tert*-butyl)oxazol-2-yl)methyl)thio)thiazol-2-yl)-1-(4-((2-(2,6-dioxopiperidin-3-yl)-1,3-dioxoisoindolin-4-yl)thio)butyl)piperidine-4-carboxamide (**25**). Yellow solid (27.9 mg, 55%). ^{1}H NMR (400 MHz, DMSO-*d*$_6$) δ 12.44 (s, 1H), 11.14 (s, 1H), 9.66 (s, 1H), 7.87 – 7.75 (m, 2H), 7.70 – 7.58 (m, 1H), 7.41 (d, *J* = 4.6 Hz, 1H), 6.72 (d, *J* = 1.8 Hz, 1H), 5.13 (dd, *J* = 12.7, 5.4 Hz, 1H), 4.07 (s, 2H), 3.55 (d, *J* = 11.6 Hz, 2H), 3.21 (t, *J* = 7.0 Hz, 2H), 3.11 (s, 2H), 2.99 – 2.84 (m, 3H), 2.74 (d, *J* = 12.0 Hz, 1H), 2.61 (d, *J* = 20.3 Hz, 1H), 2.56 – 2.52 (m, 1H), 2.05 (d, *J* = 12.4 Hz, 3H), 1.90 (dd, *J* = 24.6, 10.6 Hz, 4H), 1.73 (d, *J* = 6.8 Hz, 2H), 1.19 (s, 9H). MS (ESI) m/z: calcd. for $C_{34}H_{41}N_6O_6S_3^+$ $[M+H]^+$, 725.22; found 725.3.

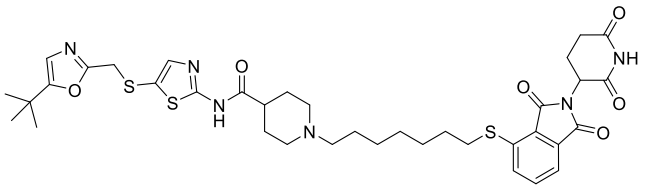

N-(5-(((5-(*tert*-butyl)oxazol-2-yl)methyl)thio)thiazol-2-yl)-1-(7-((2-(2,6-

dioxopiperidin-3-yl)-1,3-dioxoisoindolin-4-yl)thio)heptyl)piperidine-4-carboxamide (**26**). Yellow solid (33.8 mg, 63%). ^{1}H NMR (400 MHz, DMSO-d_6) δ 12.44 (s, 1H), 11.13 (s, 1H), 9.98 (s, 1H), 7.78 (dt, J = 16.5, 8.1 Hz, 2H), 7.64 (d, J = 7.0 Hz, 1H), 7.41 (d, J = 3.4 Hz, 1H), 6.73 (d, J = 6.5 Hz, 1H), 5.12 (dd, J = 12.7, 5.4 Hz, 1H), 4.04 (d, J = 19.6 Hz, 2H), 3.53 (d, J = 10.5 Hz, 2H), 3.15 (t, J = 7.1 Hz, 2H), 3.06 – 2.98 (m, 2H), 2.96 – 2.83 (m, 3H), 2.74 (dd, J = 21.0, 9.4 Hz, 1H), 2.60 (d, J = 19.4 Hz, 1H), 2.57 – 2.52 (m, 1H), 2.09 – 1.87 (m, 5H), 1.68 (d, J = 6.8 Hz, 4H), 1.47 (s, 2H), 1.33 (s, 4H), 1.21 (d, J = 17.8 Hz, 9H). MS (ESI) m/z: calcd. for $C_{37}H_{47}N_6O_6S_3^+$ $[M+H]^+$, 767.27; found 767.3.

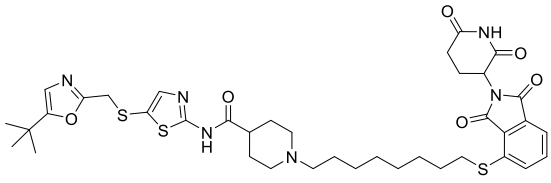

N-(5-(((5-(*tert*-butyl)oxazol-2-yl)methyl)thio)thiazol-2-yl)-1-(8-((2-(2,6-dioxopiperidin-3-yl)-1,3-dioxoisoindolin-4-yl)thio)octyl)piperidine-4-carboxamide (**27**). Yellow solid (36.1 mg, 66%). ^{1}H NMR (400 MHz, DMSO-d_6) δ 12.43 (s, 1H), 11.13 (s, 1H), 9.77 (s, 1H), 7.78 (dt, J = 16.4, 8.0 Hz, 2H), 7.64 (d, J = 6.9 Hz, 1H), 7.41 (d, J = 3.5 Hz, 1H), 6.73 (s, 1H), 5.12 (dd, J = 12.8, 5.4 Hz, 1H), 4.07 (s, 2H), 3.54 (d, J = 11.8 Hz, 2H), 3.14 (t, J = 7.2 Hz, 2H), 3.02 (d, J = 6.3 Hz, 2H), 2.95 – 2.83 (m, 3H), 2.73 (dd, J = 24.9, 13.0 Hz, 1H), 2.60 (d, J = 19.5 Hz, 1H), 2.55 – 2.52 (m, 1H), 2.05 (dd, J = 13.9, 9.7 Hz, 3H), 1.91 (dd, J = 23.5, 11.9 Hz, 2H), 1.68 (d, J = 6.9 Hz, 4H), 1.46 (s, 2H), 1.32 (s, 6H), 1.19 (s, 9H). MS (ESI) m/z: calcd. for $C_{38}H_{49}N_6O_6S_3^+$ $[M+H]^+$, 781.29; found 781.3.

References

1. Wu, Y. *et al.* Ubiquitin ligase E3 HUWE1/MULE targets transferrin receptor for degradation and suppresses ferroptosis in acute liver injury. *Cell Death Differ* **29**, 1705-1718 (2022).
2. Stuart, T. *et al.* Comprehensive Integration of Single-Cell Data. *Cell* **177**, 1888-1902 e1821 (2019).
3. Han, X. *et al.* Construction of a human cell landscape at single-cell level. *Nature* **581**, 303-309 (2020).
4. Tirosh, I. *et al.* Dissecting the multicellular ecosystem of metastatic melanoma by single-cell RNA-seq. *Science* **352**, 189-196 (2016).